



Comparative Performance Test of an Inclinometer Wireless Smart Sensor Prototype for Subway Tunnel

Hongwei Huang^{1,2,*}, Ran Xu^{1,2}, Wei Zhang^{1,2}

¹Key Laboratory of Geotechnical and Underground Engineering of Minister of Education,
Tongji University, Shanghai 200092, China

²Department of Geotechnical Engineering, Tongji University, Shanghai 200092, China

Abstract: Structural health monitoring of operating subway tunnel has become a new challenge to engineers. In order to make structural monitoring cheaper, smarter and more efficient, new technologies such as micro-electro-mechanical system (MEMS) sensors and wireless sensor network (WSN) have recently been introduced to compensate the defects of conventional methods. A wireless MEMS inclinometer prototype was developed by Tongji University. Many adaptability tests on both developed and commercial sensors are carried out in laboratory under the same condition. The comparison shows that the inclinometer prototype has a higher resolution, larger range, lower cost, better electric property and less temperature disturbance than the commercial product but is slightly bigger in size. Then, a full size shield tunnel segment deformation experiment is carried out. Tilt angles at some particular locations are measured by the MEMS inclinometers so as to calculate the global deformation of the segment. Conventional displacement meter is used to verify the calculated results. The feasibility of utilizing inclination of segments to evaluate convergence deformation of shield tunnel is studied in this paper. The geometry method is adopted in analysis, and the convergence deformation of shield tunnel is assumed as a function of segments inclination. The experiment shows a solid feasibility of inclinometers being used to monitor convergence displacement of shield tunnel. Problems discovered in the research and future work are also discussed.

Keywords: Smart sensor, MEMS, shield tunnel, convergence deformation

DOI: [10.7492/IJAEC.2013.003](https://doi.org/10.7492/IJAEC.2013.003)

1 INTRODUCTION

Over the last few years, China has experienced a rapid expansion of urban territory. Consequently, residential areas have become further and further from city centers. Chinese answer to this problem is to connect uptown and downtown area with urban railway transit. At the end of 2011, the mileage of Chinese urban railway transit has reached 1644.9km and is still growing rapidly (Gu 2012).

As the metro network expanding, some problems also emerge. Many sections of subway tunnels have suffered from various degrees of structural defects due to factors like poor soil condition, construction deficiency, adjacent construction and so on. A study in 2009 showed more than 20,000 spots of leakage and more than 400 spots of cracks spread around the Shanghai metro net-

work. In some areas, large deformation is also detected. Concrete ageing problem is also found in some older tunnels. Therefore, how to monitor the status of operating tunnels effectively and how to maintain a tunnel network so large in scale become a new challenge to Chinese engineers (Wang and Xiao 2012).

China has also spent a lot of money in maintenance of subway tunnels. But the technologies and methods we using are not so efficient. One way of convergence measurement is using servo type total station to scan the surface of the tunnel. Another way is to measure convergence displacement directly by a distance meter. These conventional methods can provide convergence displacement data with enough accuracy but they are too expensive and inconvenient to operate. As for settlement measurement, there are conventional methods like precise leveling, trigonometric leveling, hydrostatic

*Corresponding author. Email: huanghw@tongji.edu.cn

leveling, and electronic spirit level. These methods are proven technique and widely used in structural monitoring. Some new technologies such as digital imaging measurement and 3D laser scanning measurement are also emerging nowadays, which can realize automatic measurement to a certain extent but they are highly expensive (Li et al. 2011).

As the current situation of structural health monitoring, most works including detection of structural defects and deformation measurement are done by people with very primitive and inaccurate equipment. The information gathered from the site is neither standardized nor computerized which makes data processing time-consuming. Most importantly, most procedures we are taking nowadays focus on repairing and preventing further damage after the structure is already injured, instead of detecting and alerting the potential risk and taking precautions (Iwasaki 2009). These defects make conventional methods of structural health monitoring unable to meet the needs of China.

In recent years, some new sensor technologies have emerged which may largely improve the efficiency of structural health monitoring. Two of which we are particularly interested in are micro-electro-mechanical systems (MEMS) and wireless sensor network (WSN) because their characteristics are particularly suitable for the tunnel environment. MEMS are small integrated devices or systems that combine electrical and mechanical components varied in size from micrometers to millimeters (Varadan and Varadan 2000). As the technology evolving, MEMS sensors have become more integrated and less power-consuming which is ideal for its combination with WSN. Bennett et al. (2010) have applied several WSN trial systems in London, Barcelona and Prague subway tunnels. The battery powered sensor modules are small, completely wireless and easy to install. They automatically construct the network topology and acquire high quality live data 24 hours a day. These new technologies showed a great advantage over conventional methods.

2 TONGJI MEMS INCLINOMETER PROTOTYPE

As a part of Tongji's smart sensor program, TJ-UWIS is a series of MEMS inclinometer prototypes developed by the College of Electronics and Information Engineering, Tongji University. The chip selection,

schematic design, PCB layout and parameter optimization were all done by specialists from Tongji. Three different specifications of TJ-UWIS sensors are provided for various purposes. There are single axis analog inclinometer (V1.3), dual axis analog inclinometer (V1.1) and single axis differential inclinometer (V1.2). The TJ-UWIS is compatible with our own wireless smart sensor network which is still under development. Meanwhile, a commercial MEMS inclinometer product is chosen as a comparison.

A series of tests are conducted in order to inspect the MEMS sensor's adaptability to various environments. All the sensors are tested under the same condition to compare their performances. The performance indexes in Table 1 show that the TJ-UWIS prototype has higher precision, better resolution, larger range, less cost and wider working temperature range than the commercial product. But it is slightly bigger due to compatibility requirements.

The TJ-UWIS prototype will be improved through a series of laboratory and field tests. In the future, the final product will be used in the smart sensing system for the urban railway transit.

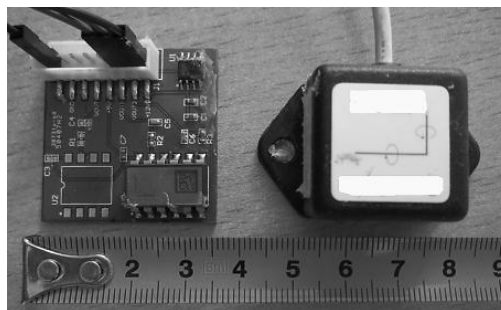


Figure 1. TJ-UWIS prototype and commercial inclinometer

3 PERFORMANCE TEST

3.1 Temperature Drift Test

A unique feature of MEMS sensors is their sensitivity to the temperature change. Some field tests of MEMS sensors have shown significant data shift due to air temperature (Soga 2010). The inclination based convergence measurement method requires extremely stable output and high accuracy from the inclinometer because the calculation process has significantly amplified the disturbance. Although most MEMS sensors

Table 1. Performance index

	Axis	Size (mm)	Precision (°)	Resolution (°)	Range (°)	Input voltage (V)	Output voltage (V)	Working temperature (°C)
Commercial Sensor	1	27×27	0.5	0.03	-20~20	6~30	0~5	-40~85
TJ-UWIS (V1.1)	2	35×35	0.1	0.0025	-90~90	12	0~5	-40~125
TJ-UWIS (V1.2)	1	35×35	0.1	0.0013	-30~30	12	0~5	-40~125
TJ-UWIS (V1.3)	1	35×35	0.1	0.0025	-30~30	12	0~5	-40~125

Table 2. Temperature drift test

	Axis	Output voltage (V)		Datum drift	Datum drift
		0°C	70°C	(V)	(°)
Commercial sensor	X	1.3127	1.3257	0.013	0.264
	Y	1.3263	1.3442	0.0179	0.352
TJ-UWIS (V1.1)	X	1.2187	1.2269	0.0082	0.495
	Y	1.2571	1.2639	0.0068	0.407

are altered to minimize the temperature drift, the influence of the temperature change still cannot be ignored which will be shown in this test.

A temperature test chamber is used to control the temperature. Two MEMS sensors are chosen and tested in the same condition. After being fitted in the chamber, they remain still throughout the test. The temperature first drops to 0°C and then gradually rises to 70°C. The whole process lasts about 45 minutes. The outputs of the sensors are monitored and the extreme values occur at poles of the temperature.

The test result in Table 2 shows that the temperature change has a clear influence on both sensors. The output voltage drift of TJ-UWIS (V1.1) is much less than the commercial sensor indicating that it has a better electric property. Contrarily, the drift of TJ-UWIS (V1.1) measured by degree is relatively larger due to a much larger range. This problem can be fixed by adding a temperature compensation module, improving the electric property of the PCB and lowering the range of the sensor.

3.2 Power Consumption Test

The TJ-UWIS sensor module is designed for the wireless sensor network. The capacity of its battery power is limited. It is important to evaluate the module's power consumption so as to better allocate battery energy.

This test intends to compare the power consumption of the two inclinometers. In each round of tests, the sensors will be installed on a static platform. Then, it will keep collecting data at a certain rate until its 55 mAH battery is dead. The battery duration of each sensor under the data rate of 1 sec and 3 sec is listed in Table 3. It appears that the commercial sensor has a better overall power consumption performance than TJ-UWIS (V1.1). Especially when the data rate is lowered, its battery life extended significantly. The result indicates the necessity of adding a power management module to the TJ-UWIS prototype for better energy saving.

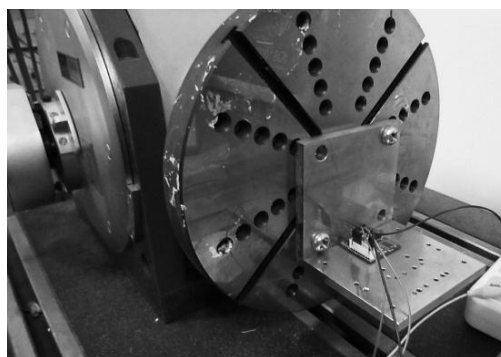
Table 3. Power consumption test

	Sample interval	Duration	Data number
Commercial sensor	1 sec	260 min	12700
	3 sec	310 min	5850
TJ-UWIS (V1.1)	1 sec	235 min	11500
	3 sec	230 min	4300

3.3 Calibration

In order to determine the output curve of TJ-UWIS sensors, a circular dividing table is used to precisely control the angle of the sensor (Figure 2). The accuracy of the circular dividing table is 2". During each calibration, the table will rotate 5 ~ 10° a time until the range of the inclinometer is covered. The angle and output voltage are measured by a sampling instrument with high accuracy. The result of calibration is shown in Figure 3 and Table 4.

In summary, the linearity of TJ-UWIS prototypes and the commercial sensors are all acceptable. All the output curves are reasonably linear and smooth within their ranges.

**Figure 2.** Circular dividing table

4 INCLINATION BASED CONVERGENCE DEFORMATION MEASURING METHOD FOR SHIELD TUNNEL

4.1 Geometry Model of Shield Tunnel Deformation

Jointed segmental precast concrete linings connected by steel bolts are commonly used in most shield-driven tunnels. The segments are prefabricated in factories and assembled in the sites. The strength of segment concrete is usually above C50. This kind of structure results in less stiffness and larger deformation of joints compared with concrete segments. The opening of joints causes segments rotation, and convergence deformation is embodied in the whole lining ring. So the convergence deformation of the shield tunnel can be determined by the segment inclination.

As the lining of a shield-driven tunnel is not a continuous ring structure due to the existence of joints,

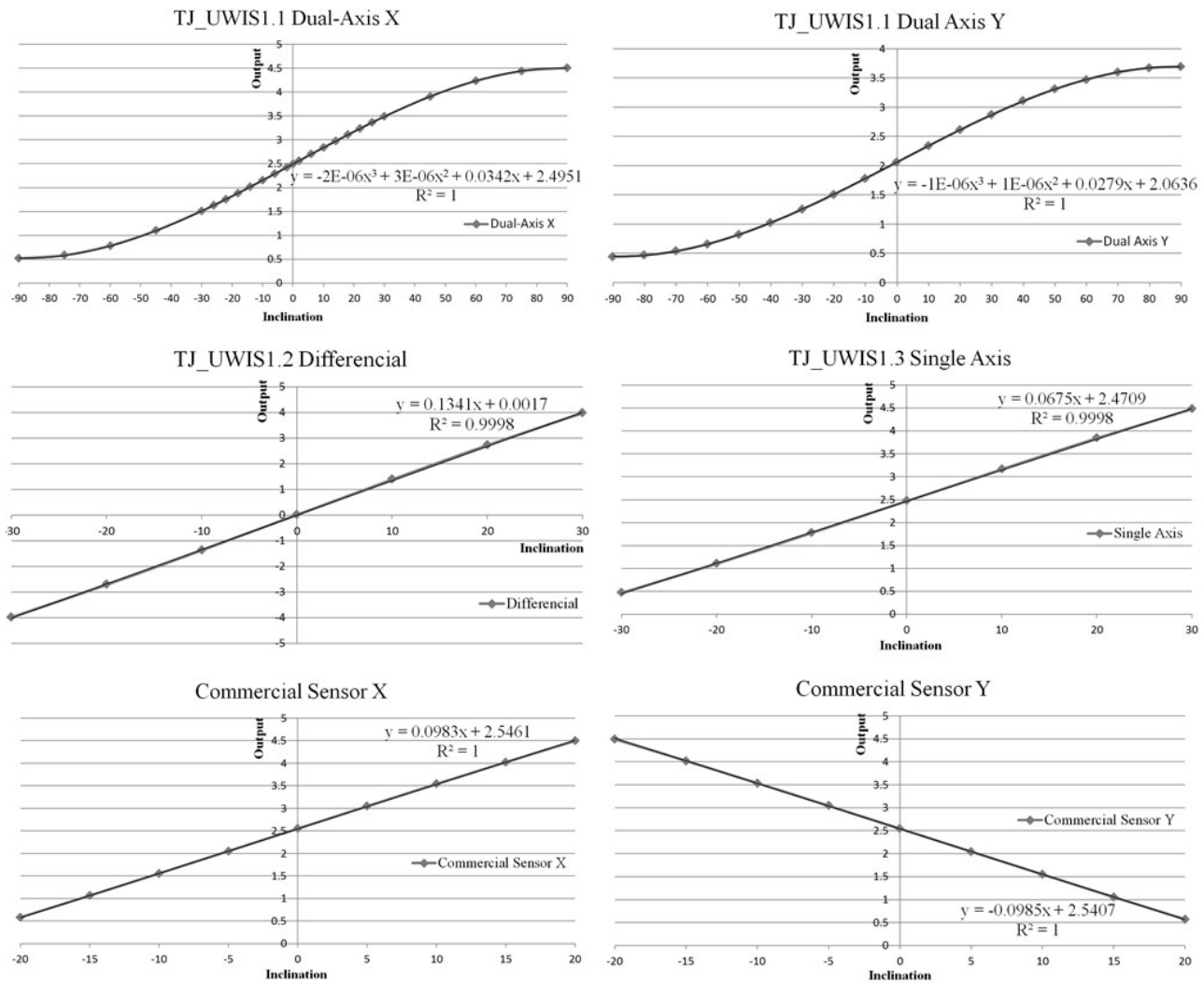


Figure 3. Output curve of inclinometers

different models should be used to simulate segments and joints. This paper proposed a geometry model to describe the deformation in the cross section. In this model, the touching points of joints are simulated by base points, and the connection of adjacent base points (base line) is used to represent the segment. In the deformation process, the opening of joints can be reflected by the change of the base angle between the adjacent base line, and the segment rotation can be reflected by the base line rotation, as the Figure 4 shows.

There are two main assumptions about the geometry model. Firstly, the length of baseline L is assumed

to be a constant value in analysis. Secondly, the base points refer to the endpoints of joints which are in the compressive zone. From the geometry point, if the degree of the base angle and the length of the baseline are known, the relative displacement between base points is determined.

4.2 Determination of Interior Angle and Inclination Measurement

The key point is how to get the base angle. It is unrealistic to utilize inclinometer to measure the angle

Table 4. Calibration results

Sensor	Axis	Output curve	R^2
TJ-UWIS (V1.1)	X	$V = -2E-06a^3 + 3E-06a^2 + 0.0342a + 2.4951$	1
	Y	$V = -1E-06a^3 + 1E-06a^2 + 0.0279a + 2.0636$	1
TJ-UWIS (V1.2)	X	$V = 0.1341a + 0.0017$	0.9998
TJ-UWIS (V1.3)	X	$V = 0.0675a + 2.4709$	0.9998
Commercial sensor	X	$V = 0.0983a + 2.5461$	1
	Y	$V = -0.0985a + 2.5407$	1

Note: V : Output voltage; a : Inclination angle

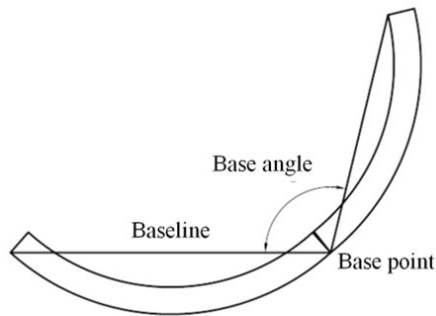


Figure 4. Geometry model of shield tunnel deformation

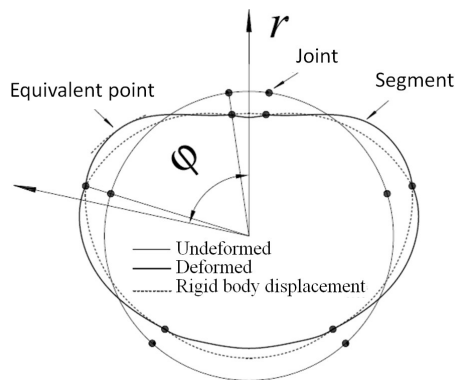


Figure 5. The concept of equivalent point

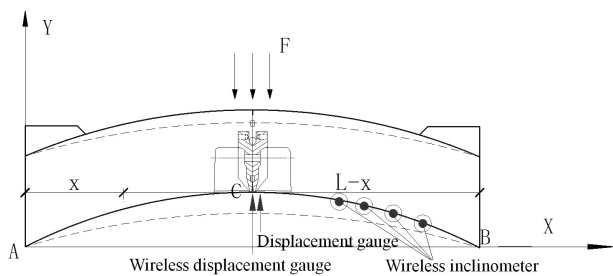


Figure 6. Schematic diagram of the test structure

directly. However, the rotation of segments can be detected by inclinometer quite precisely. With the initial base angle, the value of the base angle can be recorded during the deformation process.

Using the geometry model to evaluate the convergence deformation implies an assumption that the segments are considered as a rigid body which is unable to deflect and the displacement of segment is only caused by the joint opening. It is too rough to calculate.

Actually, the inclination of a segment includes two parts, which are the rigid body rotation caused by the joint opening and the deflection of segment caused by the internal force, mainly bending moment. In the geometry model, only rigid body rotation should be taken into deformation calculation. So proper method should be adopted to extract rigid body rotation from the inclination of segments which is measured by inclinometer.

To solve this problem, the concept of equivalent point is proposed. Equivalent point refers to the point in segment where the angle displacement is zero, as shown in Figure 5. As a result, if the equivalent point can be found, the rigid body rotation can be measured from segments, and the convergence deformation can be described.

Based on the equation of beam deflection curve, for each segment, the segment deflection can be solved by the following equation:

$$\frac{d^2r}{R^2d\varphi^2} = \frac{M(\varphi)}{EI}$$

$$r(\varphi_{j1}) = a$$

$$r(\varphi_{j2}) = b$$

where $r(\varphi_{j1}) = a$, $r(\varphi_{j2}) = b$ refer to the rigid body displacement, and R is the radius of segment ring.

Deflection angle and displacement can be got after the equation is integrated once and twice. To solve the equivalent point position, the rigid body displacement should be eliminated and the Eq. (1) can be transformed as:

$$\frac{d^2r_s}{R^2d\varphi^2} = \frac{M(\varphi)}{EI}$$

$$r_s(\varphi_{j1}) = 0$$

$$r_s(\varphi_{j2}) = 0$$

where r_s refers to the deflection caused by segment deformation. And the position of equivalent point can be found by solving the following equation:

$$\left. \frac{dr_s}{Rd\varphi} \right|_{\varphi=\varphi_e} = 0$$

where φ_e refers to the position of equivalent point.

4.3 Test of the Algorithm on Segment-joint Structure

To study the feasibility of monitoring in tunnel based on a wireless sensor network, Li et al. (2012) conducted a laboratory test on segment-joint structure including deflection and inclination measurement. A schematic diagram of the test structure is shown in Figure 6.

A traditional displacement gauge is installed in the mid-span of the segment structure. A wireless inclinometer is installed on the segment with different positions each time. The segment is loaded and unloaded repeatedly, and the deflection and inclination are recorded.

With the given load, the bending moment of the structure can be determined as:

$$M(x) = \begin{cases} \frac{Fx}{2}, & (0 < x \leq \frac{L}{2}) \\ \frac{F(L-x)}{2}, & (\frac{L}{2} < x < L) \end{cases} \quad (4)$$

where F is a vertical concentrated force applied by hydraulic jacks, and L is the horizontal length of the segment test piece.

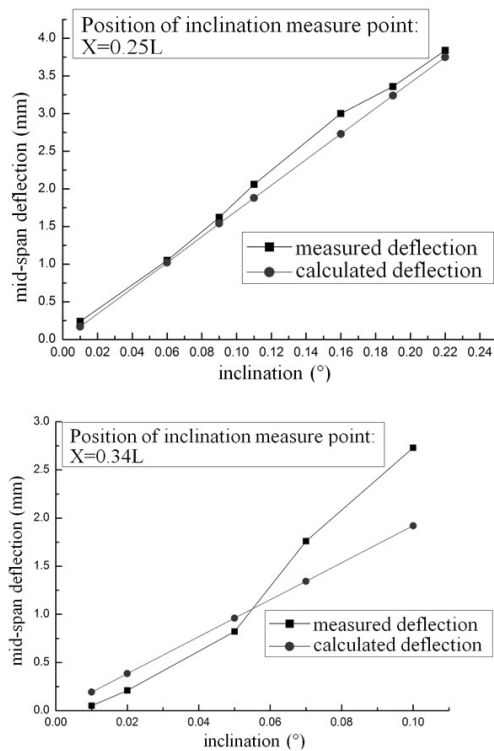


Figure 7. Deflection comparisons

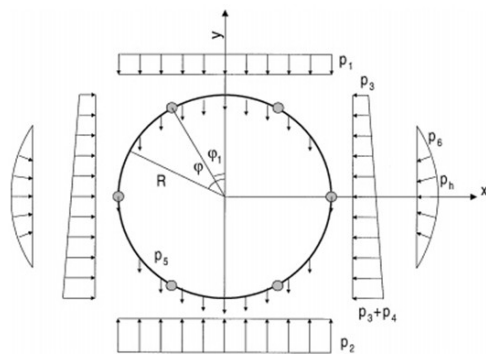


Figure 8. Load distribution model of shield tunnel

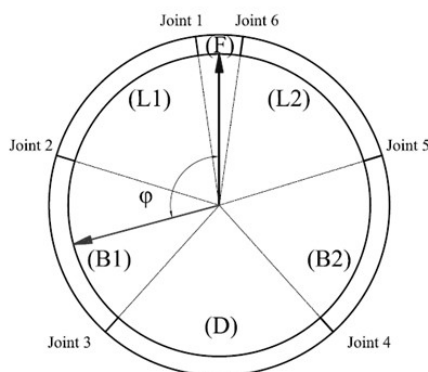


Figure 9. Lining cross-section of Shanghai metro tunnel

According to the present mathematical model, the equivalent points in the test model lay on the position where $x = 0.28L$. And the mid-span angular deflection ω can be calculated as:

$$w = \frac{L}{2} \tan \alpha \quad (5)$$

where α refers to the inclination of segment.

In the test, inclination measure points lay on the positions where $x = 0.25L$ and $x = 0.34L$. And the measured inclinations in the test are used to calculate the displacement in mid-span. The comparison between the calculated results and the measured deflection is shown in Figure 7.

As the comparison showed, the measure point which is close to the equivalent point (where $x = 0.28L$) gives the better accuracy of calculation and the error can be accepted in structure monitoring.

4.4 Analytical Solution of the Equivalent Point

To find the equivalent points needs the accurate prediction of bending moment distribution around the tunnel lining. To predict the bending moment distribution around a jointed segmental precast circular tunnel lining, an analytical solution based on the “force method” is used in analysis (Lee et al. 2001).

Based on the field observation of earth pressure distributions acting around segmental tunnels in soft clay, the earth pressures can be expressed as illustrated in Figure 8. Here p_6 is assumed to be distributed over the range of $45^\circ - 135^\circ$ with respect to the vertical direction around the tunnel and to act perpendicularly to the tunnel with a parabolic pattern as defined by the following equation:

$$p_6 = K_s \Delta_h (1 - 2 \cos^2 \varphi) \quad (6)$$

where K_s is the soil resistance coefficient and Δ_h is the horizontal displacement at the spring line of the tunnel.

In the proposed analytical solution, the radius of the tunnel is taken as R ; the rigidity of the lining segment (per unit length) is taken as EI . The flexural stiffness of the joint, K_θ , is assumed to be a constant value. A dimensionless parameter called as the joint stiffness ratio, $\lambda = K_{\theta l}/EI$, is introduced to represent the relative stiffness of the joint over the rigidity of the lining segment. The calculation length, l , is usually taken as $1m$ to represent a typical unit length of a lining segment.

With the structure symmetry, the force method equations can then be established by considering zero rotation and zero horizontal displacement at the crown and the invert of the tunnel. And the equations can be solved by iteration based on accordance between soil resistance pressure and the convergence deformation developed at the horizontal diameter.

Based on the Shanghai metro tunnel condition, a cross-section of the Shanghai metro tunnel is illustrated

in Figure 9. With the structure symmetry, there is no rigid body inclination developed in segments F and D. As a result, only the inclination of segments L and B should be measured and the equivalent points also need to be determined. The load distribution is determined by embedded depth and lateral pressure coefficient. The embedded depths from 5m to 25m are taken into consideration. The joints are assumed as elastic pins. And to reflect the different states of joints, 3 cases are taken into analysis, as the joint stiffness ratio of 0.03, 0.1 and 0.3 respectively. The calculated equivalent point positions are listed in Table 5.

The solution shows that the equivalent point is not fixed in a segment. However, the fluctuation of the equivalent point position is within a narrow range. In Segment L, it fluctuates from 47.9° to 56.4°. And for segment B, it fluctuates from 91.5° to 101.3°. For convenience, the mid-value of the range was selected as the measuring point.

Table 5. Calculated positions of equivalent points $\varphi_e(^{\circ})$

Embedded depth (m)	Joint stiffness ratio					
	Segment L			Segment B		
	0.03	0.1	0.3	0.03	0.1	0.3
5	47.9	51.1	53.8	91.5	97.6	98.9
10	49.3	52.8	55.7	98.6	100	100.7
15	49.7	53.2	56.2	99.6	100.5	101
20	49.9	53.5	56.4	100	100.6	101.2
25	50	53.6	56.5	100.1	100.7	101.2
30	50.1	53.7	56.6	100.3	100.8	101.3

4.5 Numerical Analysis

To verify the performance of the mathematical model, the 3D numerical analysis is adopted. Structure load model is used. The concrete segment and steel bolt are simulated with solid elements, and the soil resistance pressure is simulated by soil springs, as shown in Figure 10. Here the index of deformation is selected as the maximum convergence deformation which is usually developed between Joint 2 and Joint 5.

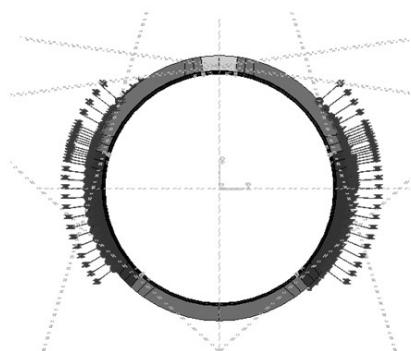


Figure 10. 3D finite element method model of Shanghai metro tunnel

With the result offered by finite element method, both the convergence deformation and the inclination at the selected measuring point can be obtained. With the inclination of segment L and segment B, the convergence deformation can be calculated and compared with the numerical results, as shown in Figure 11. It can be seen that an agreement between the numerical result and the calculated deformation is achieved.

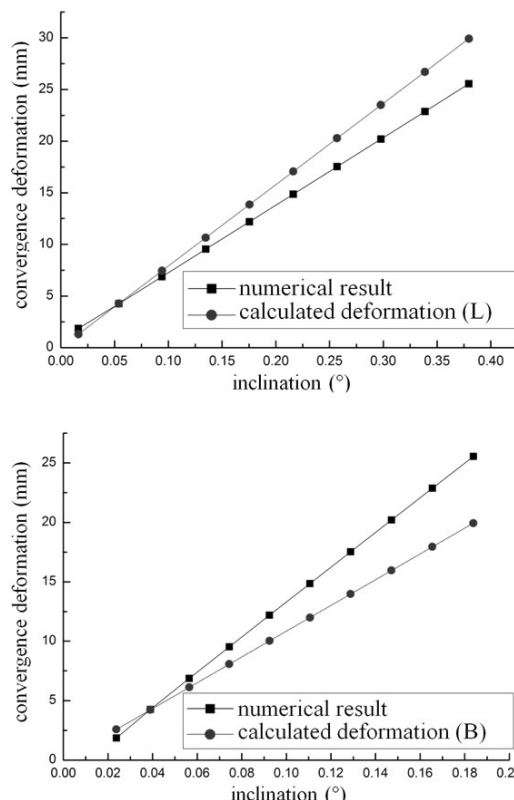


Figure 11. Convergence deformation comparisons

5 FULL SIZE SHIELD TUNNEL SEGMENT DEFORMATION EXPERIMENT

5.1 Basic Principals

As discussed above, the ring of shield tunnel is composed of several segments. The convergence displacement of shield tunnel has a functional relation with its inclination. If this function is determined, there will be a possibility to calculate the convergence displacement based on inclination.

The test-piece in this experiment is only part of a ring. The equivalent point is determined using the method introduced above. The mid-span displacement can be calculated by following equation based on inclination data (Zhang and Huang 2012).

$$a_{cs} = \frac{AC^2[\sin(\alpha_0) - \sin(\alpha_0 - I_{1s})]}{AC + BC} + \frac{BC^2[\sin(\beta_0) - \sin(\beta_0 + I_{2s})]}{AC + BC} \quad (7)$$

Table 6. Result comparison

Load level	Vertical load(kN)	Time(min)	α_{cs} (mm)	σ_{cs}	α_s (mm)	σ_s	Error(mm)	Error (%)
p1	141	43	-3.622	0.50826	-3.646	0.00023	0.0244	-0.7
P2	283	63	-2.811	1.05289	-2.599	0.00024	-0.212	7.5
P3	424	84	-1.21	0.6614	-1.187	0.0006	-0.022	1.9
P4	566	105	2.014	0.68833	1.712	0.00031	0.302	15
P5	707	126	4.309	0.35048	3.611	0.00034	0.6975	16.2
P6	849	148	6.059	1.14022	5.605	0.00014	0.4541	7.5
P7	990	168	7.98	0.7069	7.299	0.00036	0.6813	8.5
P8	1132	188	10.23	1.08599	10.212	0.00079	0.013	0.1
Average							0.242	7

where $\alpha_0 = \arctan(f/L_1)$, $\beta_0 = \arctan(f/L_2)$ as shown in Figure 12. The result will be compared with the real mid-span displacement measured by conventional instruments.

This experiment will not only verify the effect of the “inclination based convergence deformation measuring method”, but also test and compare the performance of the TJ-UWIS wireless smart sensor prototype.

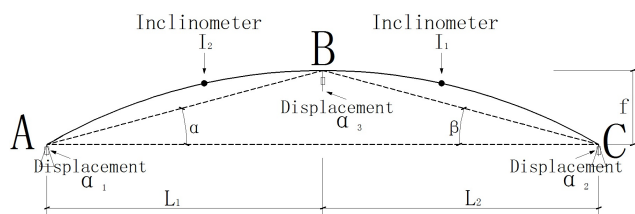


Figure 12. Sketch of the test-piece segment

5.2 Experimental Program

Figure 13 shows the experimental facility in working condition. The segment is from “Qing Cao Sha” canal tunnel. It includes two blocks of ring segment joints. The test-piece is fixed on two hinge supports which limit the linear displacement while rotation is allowed. Three horizontal hydraulic jacks are applied to simulate axial force in the ring. Vertical load is applied by a series of beams powered by another three jacks. The hydraulic jacks work in gaged mode to ensure the balance and smoothness of the forces.

There are two measuring systems in this experiment working completely independent from each other. The conventional displacement meter and foil gauge are linked by wire to the data taker which provides a reference to verify the result of the inclinometers. Meanwhile, two wireless MEMS inclinometers are installed on the undersurface of the segment. The gateway workstation (Figure 14) is set 3.5m away from the center of the segment. The line of sight between them is blocked by a steel column and the concrete segment itself. In addition, there will be personnel walking across random between the sensors and receiver during the experiment.



Figure 13. The experimental facility

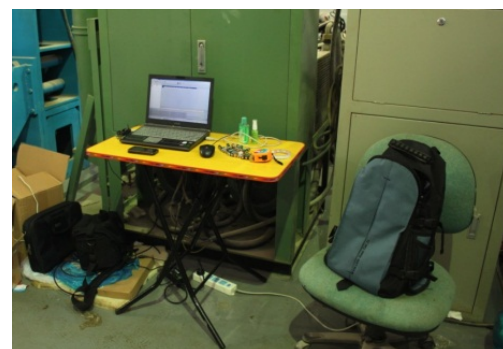


Figure 14. The gateway workstation

Table 6 shows the procedure of the load application. Two levels of axial force will first be applied. Then, eight levels of vertical load will be followed. Before each stage of force is applied, there will be a 15 min pause for the concrete segment to stabilize. Both measuring systems will record the displacement at a rate of 1 reading every 10 sec. The whole experiment will last for about 4 hours.

5.3 Results

Figure 15 and Table 6 show the calculated displacement from the wireless inclinometer (α_{cs}) and the reference displacement from conventional gauges (α_s) of each stage of load. The average error of the calculated displacement is about 7% which is acceptable. Although the variance of the calculated displacement (σ_{cs}) is relatively large, indicating that the readings of the inclinometer are shifting constantly, they still spread evenly around the true value. Therefore, the

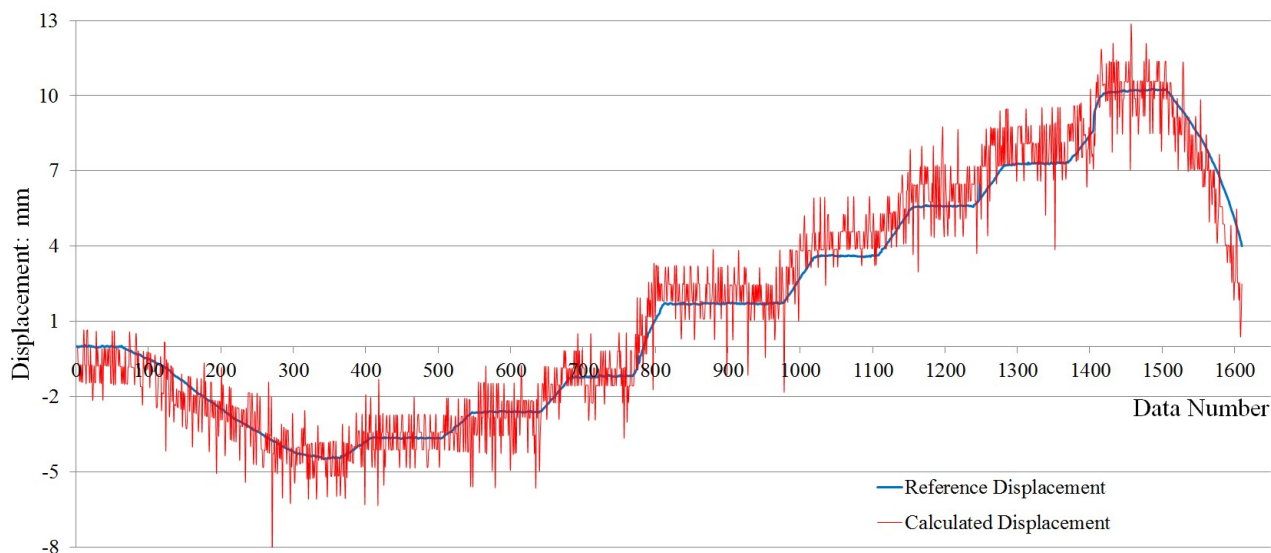


Figure 15. Recorded displacement

error can be reduced by increasing the number of readings and the calculated result can be as accurate as the reference measurement.

The wireless transmission performed well under laboratory condition. The reliability of MEMS sensor and WSN is much better than the conventional system and much easier to install and to maintain. This experiment shows a solid feasibility of this wireless MEMS inclinometer based measuring method being used for structural monitoring as an alternative.

One phenomenon we discovered in this experiment is that the displacement calculation process has significantly amplified the noise of the MEMS inclinometer which results in a high probability of false reading. We can overcome this problem by increasing the number of readings (over 50 readings per datum) during experiment. But this will cost too much time and power to get effective data. It suggests that the TJ-UWIS prototype needs further improvements.

6 CONCLUSIONS

This paper presents a mathematical model to calculate convergence deformation of shield tunnel using the inclination of segments. The concept of equivalent point was proposed to indicate the proper position for inclination measurement. To validate the feasibility of the proposed algorithm, a laboratory segment-joint structure test result is investigated, and it is shown that the inclination of equivalent point gives better accuracy in deflection calculation.

To study the application of the present mathematical model, a 3D numerical analysis is adopted. It has been demonstrated that the convergence deformation calculated by inclination of segments provides a good estimation of the numerical result. It has been found

that the method in this study is feasible to apply in shield tunnel.

TJ-UWIS (V1.1) is the first step of the smart sensor program. The full size segment deformation experiment shows the possibility of the MEMS inclinometer being used to monitor convergence displacement of shield tunnel. The comparative performance tests give us a preliminary understanding of MEMS sensors. The inclinometer prototype developed by Tongji University has a higher resolution, larger range, lower cost, better electric property and less temperature disturbance than the commercial product.

But there is still much room for improvement. A temperature compensation module and higher-performance electronic components will be necessary for MEMS sensors to reach higher accuracy. Power management is also required so as to extend battery-life. The bigger range of TJ-UWIS (V1.1) has also enlarged the disturbance and lowered the accuracy which needs reconsideration. A lot of works remain to be done before the wireless MEMS sensor can be installed into operating subway tunnels. The sensors' adaptability to harsh environment in tunnels such as dust, moisture, vibration, and radio interference needs to be tested. The robustness and long term performance of the system need to be proven.

ACKNOWLEDGEMENTS

This work was supported by the National Basic Research Program of China (2011CB013803), Natural Science Foundation Committee program (51278381) and Shanghai outstanding academic leaders program (12XD1405100). Hereby thanks to these programs. Special thanks to Professor Che Lufeng of Shanghai Institute of Microsystem and Information Technology, Chinese Academy of Sciences.

REFERENCES

- Bennett, P. J., Soga, K., Wassell, I., Fidler, P., Abe, K., Kobayashi, Y., and Vanicek, M. (2010). "Wireless sensor networks for underground railway applications: Case studies in Prague and London." *Smart Structures and Systems*, 6(5), 619–639.
- Gu, B. N. (2012). *Study of Urban Railway Transit*. Chapter Statistics of Mileage of Chinese Rrban Railway Transit in 2011. (in Chinese).
- Iwasaki, Y. (2009). "Instrumentation in ggeotechnical engineering." *Proceedings of the 17th International Conference on Soil Mechanics and Geotechnical Engineering*, TS-3A, 3288–3302.
- Lee, K. M., Hou, X. Y., Ge, X. W., and Tang, Y. (2001). "An analytical solution for a jointed shield-driven tunnel lining." *International Journal for Numerical And Analytical Methods in Geomechanics*, 25(4), 365–390.
- Li, G. H., Huang, T., Xi, G. Y., Jiang, M., and Zhang, D. (2011). "Overview on settlement monitoring of operating subway tunnels in soft clay." *Journal of Hohai University (Natural Sciences)*, 39(3), 277–284 (in Chinese).
- Li, X. J., Ji, Z., Zhu, H. H., and Gu, C. (2012). "A feasibility study on the measuring accuracy and capability of wireless sensor network in tunnel monitoring." *Frontiers of Structural and Civil Engineering*, 6(2), 111–120.
- Soga, K. (2010). "Micro-measurement and monitoring system for ageing underground infrastructure." *Contaminant Hydrology*, 94(3-4), 215–234.
- Varadan, V. K. and Varadan, V. V. (2000). "Microsensors, mmicro-electro-mechanical systems (MEMS) and electronics for smart structures and systems." *Smart Material Structures*, 9(6), 957–972.
- Wang, R. L. and Xiao, T. G. (2012). "Structural disease management and control technique of shanghai subway tunnel." *Underground Traffic and Engineering Safety*, 279–283 (in Chinese).
- Zhang, W. and Huang, H. W. (2012). "Feasibility study for evaluating convergence deformation of shield tunnel by inclination of segments." *Proceedings of the 8th International Conference on Computer Engineering and Systems*.